



Supplement of

Twenty-first-century Southern Hemisphere impacts of ozone recovery and climate change from the stratosphere to the ocean

Ioana Ivanciu et al.

Correspondence to: Ioana Ivanciu (iivanciu@geomar.de)

The copyright of individual parts of the supplement might differ from the article licence.

1 Plumb flux calculation

We use the three-dimensional flux of wave activity defined by Plumb (1985) to study the spatial patterns of planetary wave propagation. The Plumb flux is defined as follows:

$$\mathbf{F}_s = \frac{p \cos \phi}{p_o} \times \left\{ \begin{array}{l} \frac{1}{2a^2 \cos^2 \phi} \left[\left(\frac{\partial \psi'}{\partial \lambda} \right)^2 - \psi' \frac{\partial^2 \psi'}{\partial \lambda^2} \right] \\ \frac{1}{2a^2 \cos \phi} \left(\frac{\partial \psi'}{\partial \lambda} \frac{\partial \psi'}{\partial \phi} - \psi' \frac{\partial^2 \psi'}{\partial \lambda \partial \phi} \right) \\ \frac{2\Omega^2 \sin^2 \phi}{N^2 a \cos \phi} \left(\frac{\partial \psi'}{\partial \lambda} \frac{\partial \psi'}{\partial z} - \psi' \frac{\partial^2 \psi'}{\partial \lambda \partial z} \right) \end{array} \right\} \quad (1)$$

- 5 where ψ is the quasi-geostrophic streamfunction, N^2 is the buoyancy frequency, a is the radius of the Earth, Ω is the rotation rate of the Earth, ϕ and λ are the latitude and the longitude respectively, p is the pressure, with p_o taken as 1000 hPa, and the primes denote departures from the zonal mean.

2 Supplementary Figures

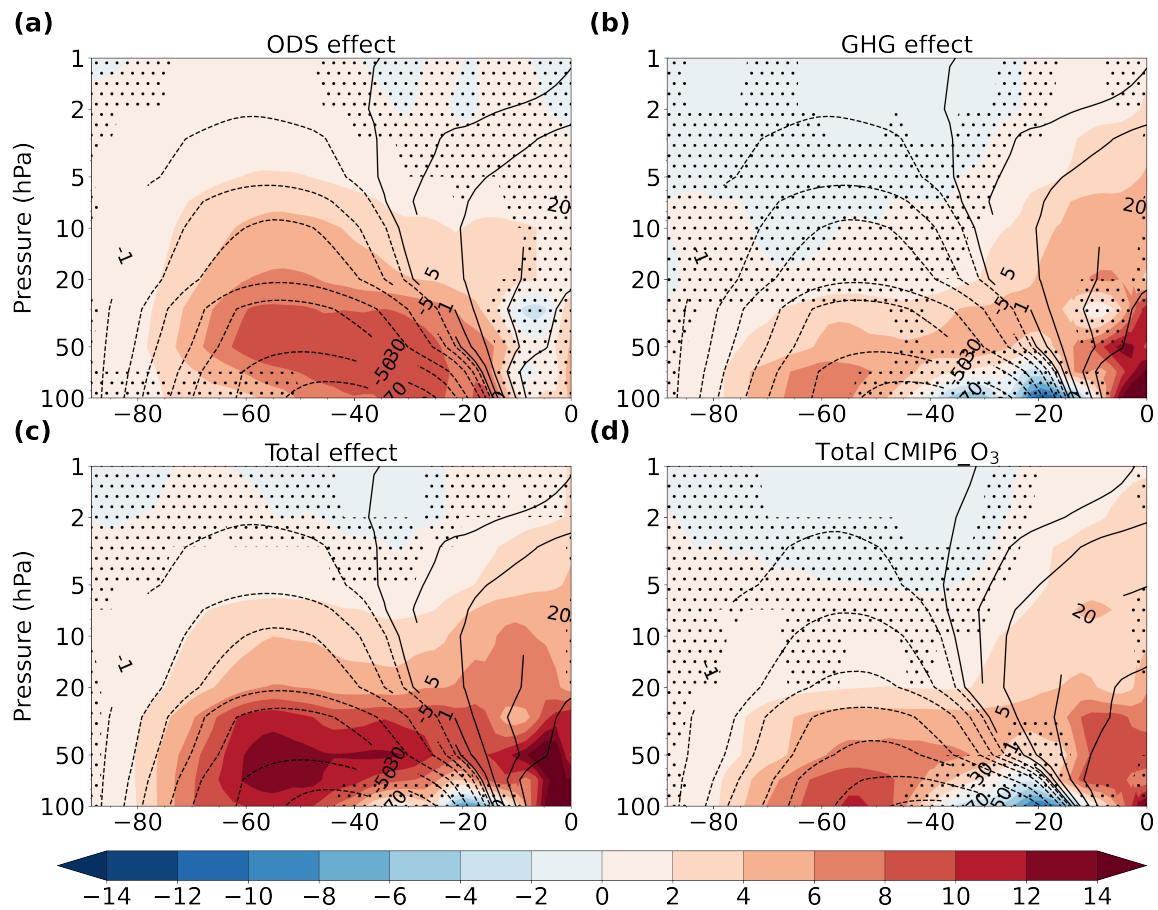


Figure S1. Changes in the mean residual streamfunction ($\text{kg m}^{-1} \text{s}^{-1}$) during November for each latitude and pressure level (color shading): effect of ozone recovery (a), effect of GHGs (b), total effect in INTERACT_O₃ (c) and total effect CMIP6_O₃ (d). The contours depict the current day (2011-2030) November climatology from INTERACT_O₃ in a-c and from CMIP6_O₃ in d. The stippling masks regions where the changes are not significant at the 95% confidence interval based on a two-tailed t-test.

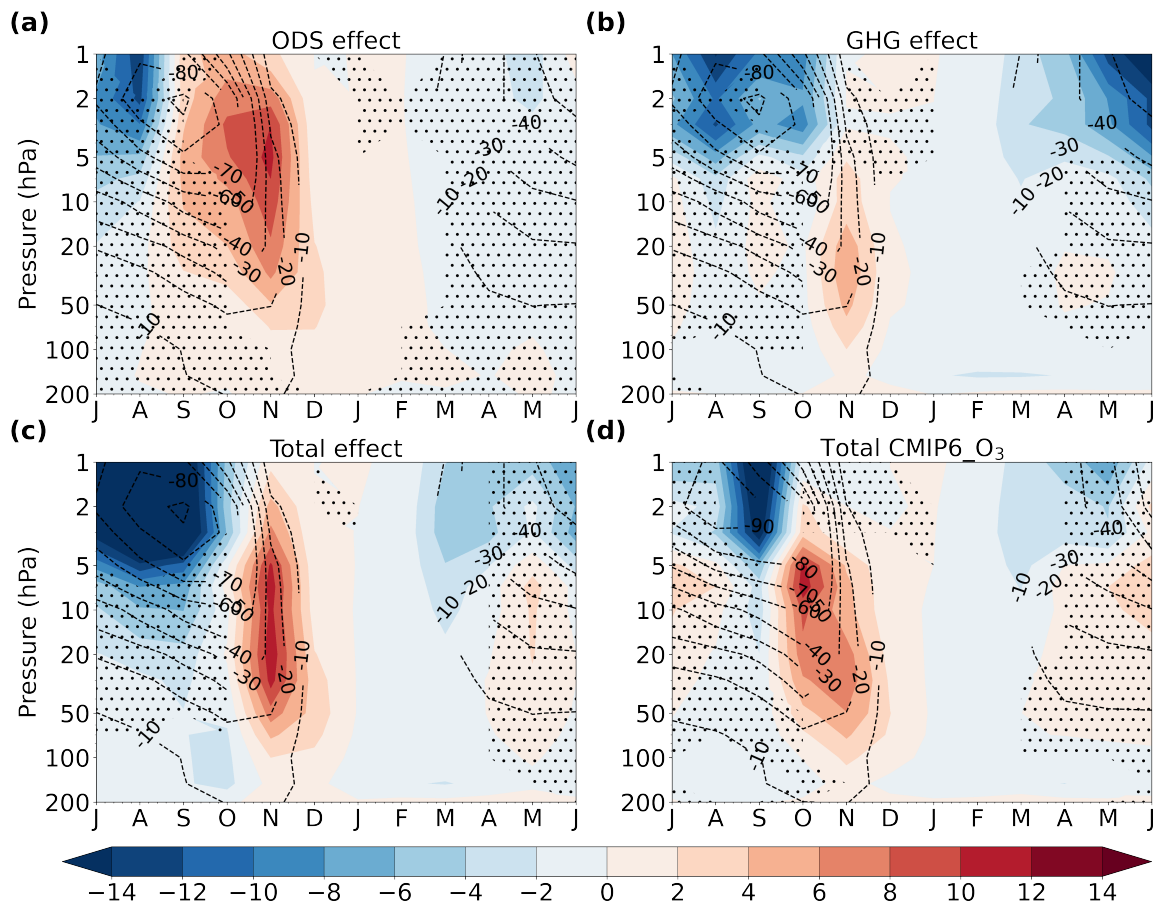


Figure S2. Changes in the eddy heat flux averaged over 45°S-80°S (kg m s^{-2}) for each month and pressure level (color shading): effect of ozone recovery (a), effect of GHGs (b), total effect in INTERACT_O₃ (c) and total effect in CMIP6_O₃ (d). The contours depict the current day (2011-2030) climatology from INTERACT_O₃ in a-c and from CMIP6_O₃ in d. The stippling masks regions where the changes are not significant at the 95% confidence interval based on a two-tailed t-test.

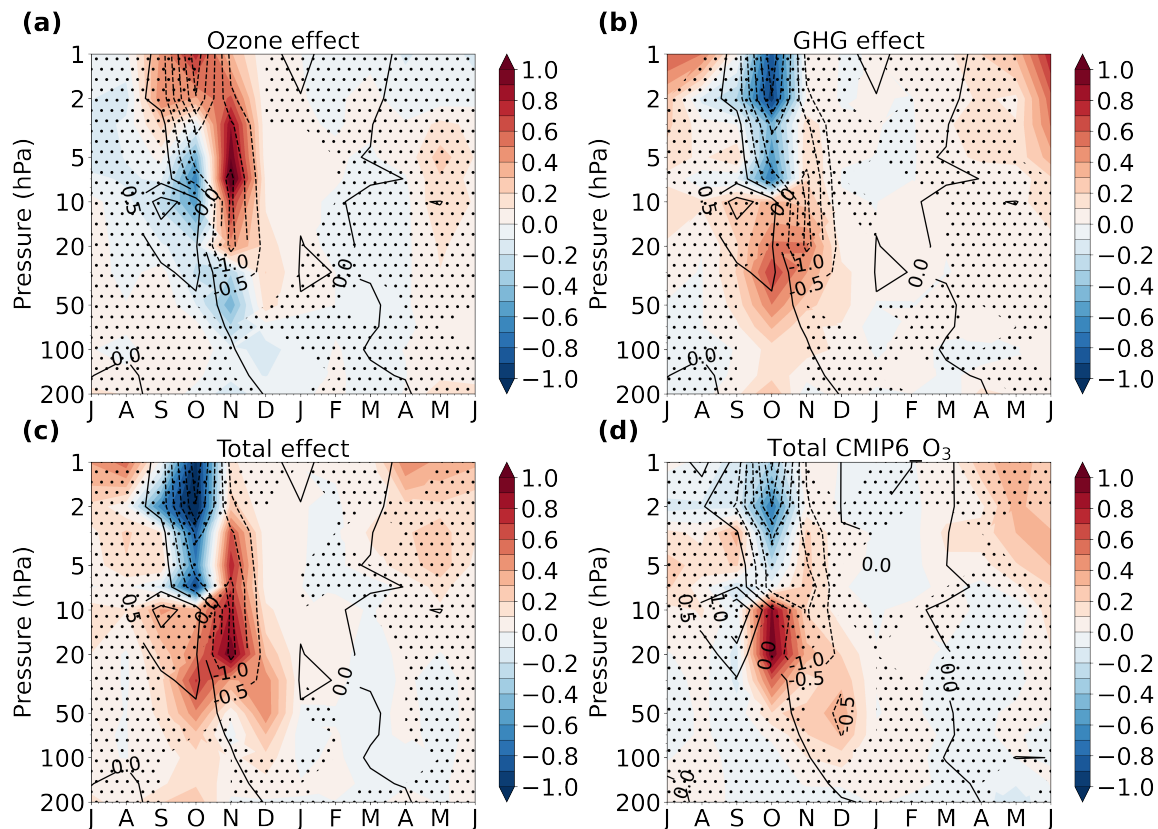


Figure S3. Changes in the divergence of the EP flux associated with the PW1 averaged over 45°S - 80°S ($\text{m s}^{-1} \text{ day}^{-1}$) for each month and pressure level (color shading): effect of ozone recovery (a), effect of GHGs (b), total effect in INTERACT_O₃ (c) and total effect in CMIP6_O₃ (d). The contours depict the current day (2011-2030) climatology from INTERACT_O₃ in a-c and from CMIP6_O₃ in d. The stippling masks regions where the changes are not significant at the 95% confidence interval based on a two-tailed t-test.

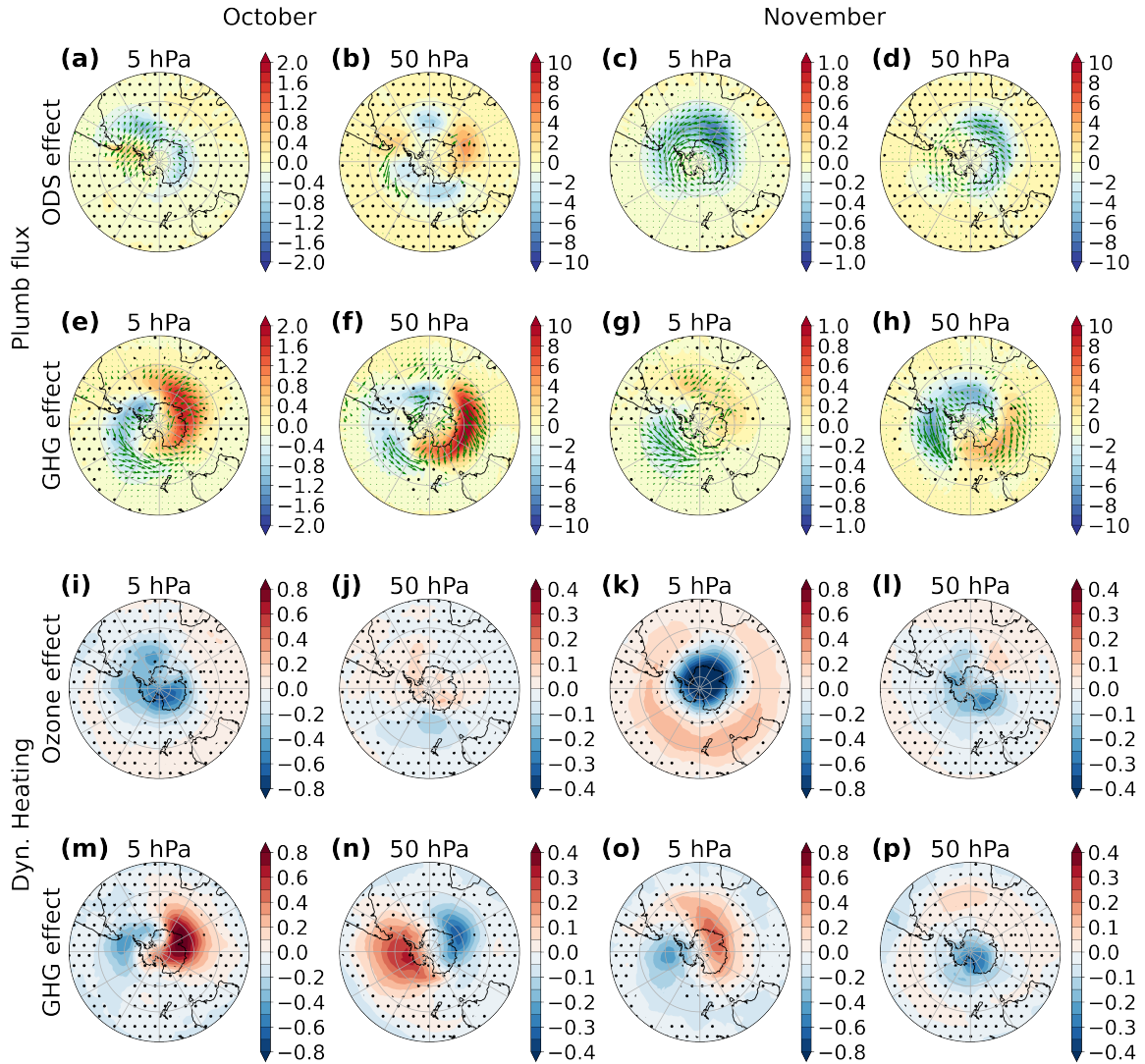


Figure S4. Changes in the flux of wave activity (a-h) and in the dynamical heating rate (i-p; K day^{-1}) at 50 hPa (b, d, f, h, j, l, n and p) and 5 hPa (a, c, e, g, i, k, m and o) during October (a, b, e, f, i, j, m and n) and November (c, d, g, h, k, l, o and p) due to ozone recovery (a-d and i-l) and increasing GHGs (e-h and m-p). The color shading in a-h shows the change in the vertical ($10^{-3} \text{ m}^2 \text{ s}^{-2}$) and the vectors show the change in the horizontal ($\text{m}^2 \text{ s}^{-2}$) component of the flux. The stippling masks regions where the changes are not significant at the 95% confidence interval based on a two-tailed t-test.

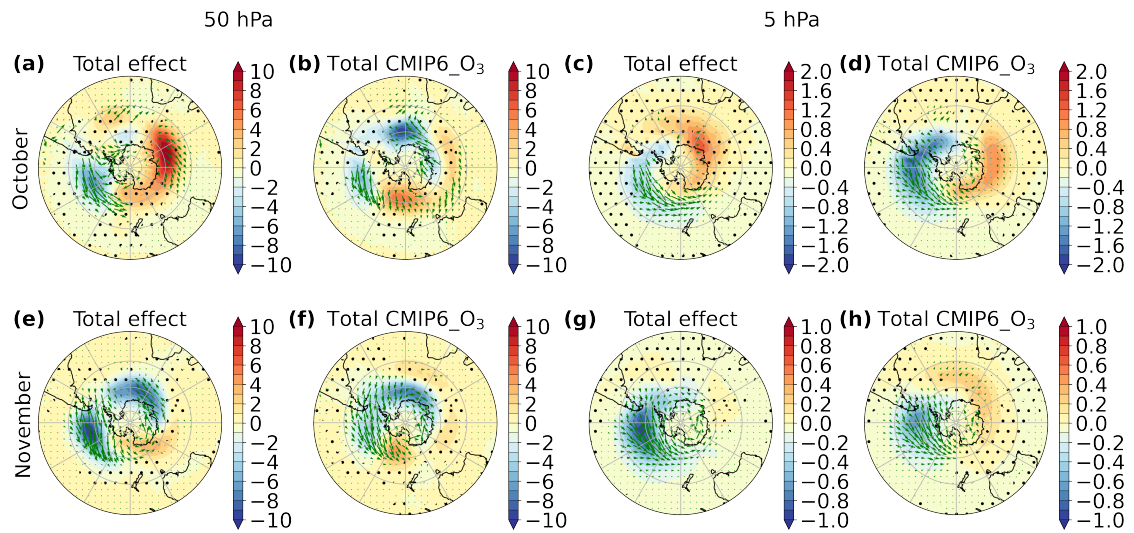


Figure S5. Changes in the flux of wave activity at 50 hPa (a, b, e and f) and at 5 hPa (c, d, g and h) during October (a, b, c and d) and November (e, f, g and h) due to ozone recovery and increasing GHGs combined, in INTERACT_O₃ (a, c, e and g) and CMIP6_O₃ (b, d, f and h). The color shading shows the change in the vertical ($10^{-3} \text{ m}^2 \text{ s}^{-2}$) and the vectors show the change in the horizontal ($\text{m}^2 \text{ s}^{-2}$) component of the flux. The stippling masks regions where the changes are not significant at the 95% confidence interval based on a two-tailed t-test.

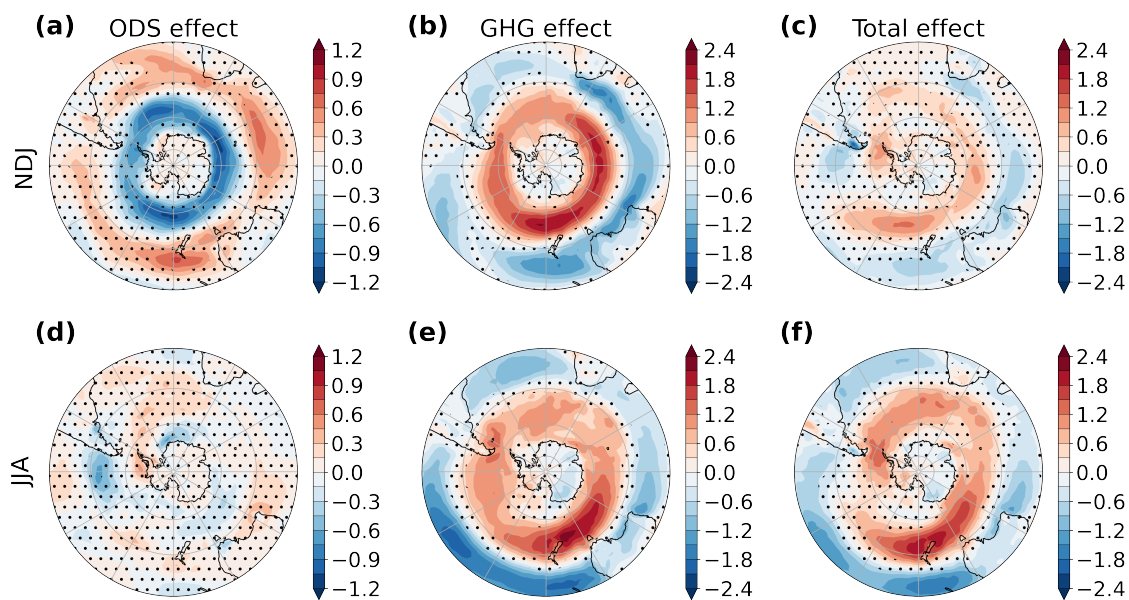


Figure S6. Changes in the surface zonal wind (m s^{-1}) during November-January (a-c) and June-August (d-f) due to ozone recovery (a and d), GHGs (b and e) and their combined effect in INTERACT_O₃ (c and f). The stippling masks regions where the changes are not significant at the 95% confidence interval based on a two-tailed t-test.

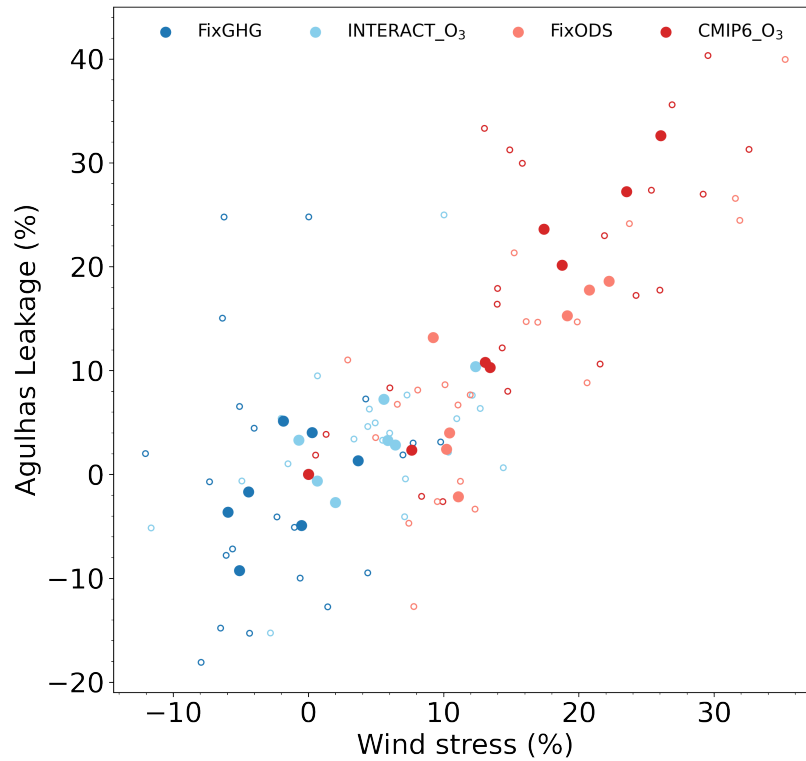


Figure S7. Decadal changes in Agulhas leakage versus decadal changes in wind stress over 45°S and 65°S and 30°E and 120°E (% change relative to 2014-2023). Each circle represents the change of each separate decade starting with 2014-2023 and ending with 2083-2094 relative to 2014-2023 in FixGHG (dark blue), INTERACT_O₃ (light blue), FixODS (light red) and CMIP6_O₃ (dark red). Filled circles denote ensemble means and small, hollow circles denote individual members.

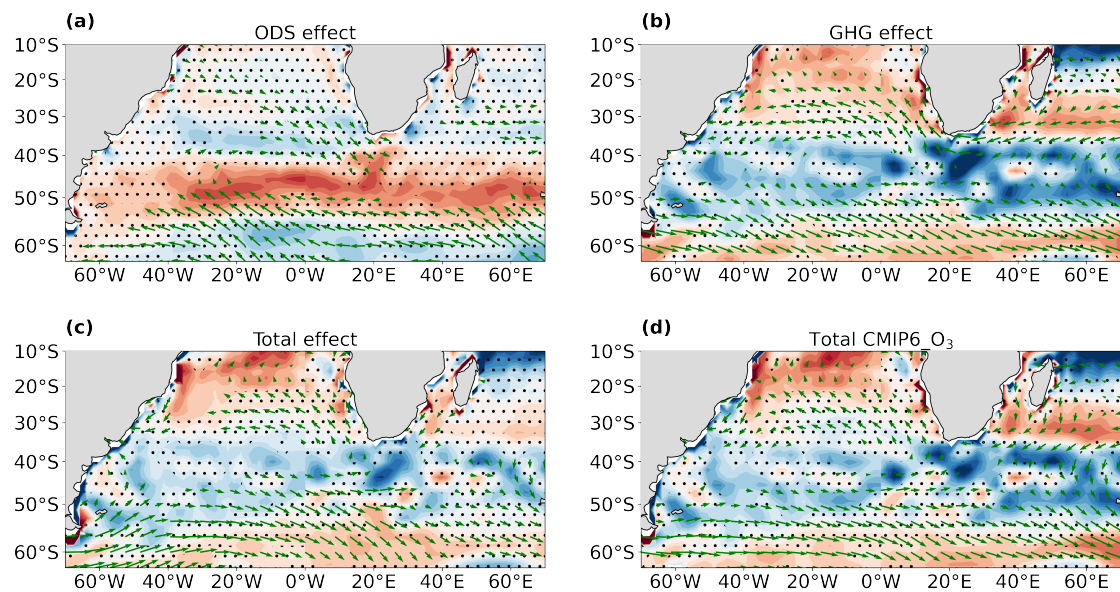


Figure S8. Changes in surface winds (arrows, in m s^{-1}) and Ekman pumping (color shading, in cm day^{-1} , positive upward) due to ozone recovery during NDJ (a), GHGs (b) and their combined effect in INTERACT_O₃ (c) and CMIP6_O₃ (d) during the entire year. Only significant (95% confidence interval) wind changes are shown and the Ekman pumping changes that are not significant are stippled.

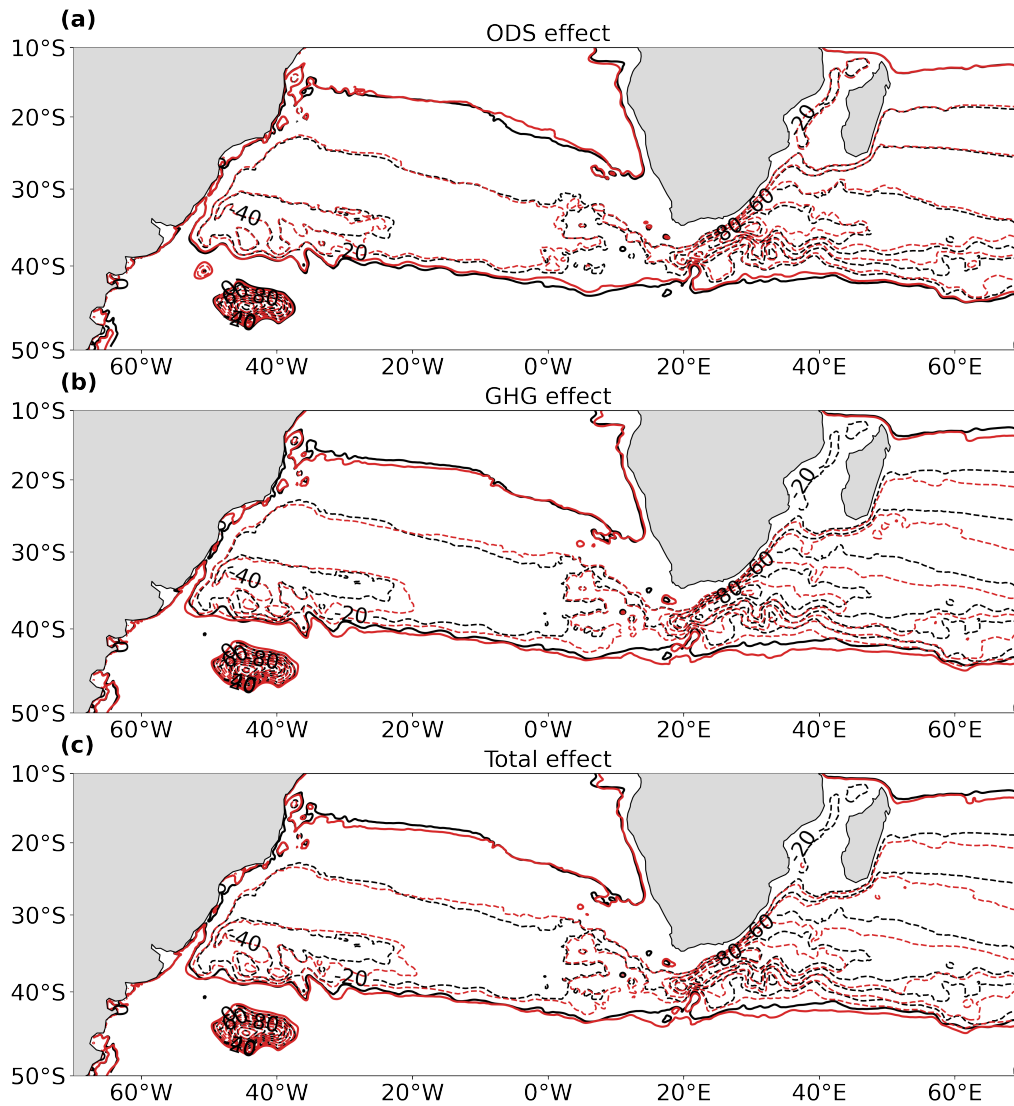


Figure S9. Changes in the subtropical gyre: the barotropic streamfunction for the current day is depicted by the black contours in all panels, while the red contours depict the streamfunction at the end of the twenty-first century in the ensemble with only ozone recovery (a), only increasing GHGs (b) and in the ensemble with both drivers (c). Only negative contours are shown and the zero contours marking the extent of the gyre is depicted by the thicker lines.